Afadin: A Key Molecule Essential for Structural Organization of Cell–Cell Junctions of Polarized Epithelia during Embryogenesis

Wataru Ikeda,* Hiroyuki Nakanishi,‡ Jun Miyoshi,‡ Kenji Mandai,‡ Hiroyoshi Ishizaki,‡ Miki Tanaka,‡ Atushi Togawa,‡ Kenichi Takahashi,‡ Hideo Nishioka,‡ Hisahiro Yoshida,§ Akira Mizoguchi,‖ Shin-ichi Nishikawa,§ and Yoshimi Takai*‡

*Department of Molecular Biology and Biochemistry, Osaka University Graduate School of Medicine/Faculty of Medicine, Osaka 565-0871, Japan; ‡Takai Biotimer Project, Exploratory Research for Advanced Technology, Japan Science and Technology Corporation, JCR Pharmaceuticals Co., Ltd., Kobe 651-2241, Japan; §Department of Molecular Genetics, Faculty of Medicine, Kyoto University, Kyoto 606-8501, Japan; and ‖Department of Anatomy and Neurobiology, Faculty of Medicine, Kyoto University, Kyoto 606-8501, Japan

Abstract. Afadin is an actin filament–binding protein that binds to nectin, an immunoglobulin-like cell adhesion molecule, and is colocalized with nectin at cadherin-based cell–cell adherens junctions (AJs). To explore the function of afadin in cell–cell adhesion during embryogenesis, we generated afadin$^{-/-}$ mice and embryonic stem cells. In wild-type mice at embryonic days 6.5–8.5, afadin was highly expressed in the embryonic ectoderm and the mesoderm, but hardly detected in the extraembryonic regions such as the visceral endoderm. Afadin$^{-/-}$ mice showed developmental defects at stages during and after gastrulation, including disorganization of the ectoderm, impaired migration of the mesoderm, and loss of somites and other structures derived from both the ectoderm and the mesoderm. Cystic embryoid bodies derived from afadin$^{-/-}$ embryonic stem cells showed normal organization of the endoderm but disorganization of the ectoderm. Cell–cell AJs and tight junctions were improperly organized in the ectoderm of afadin$^{-/-}$ mice and embryoid bodies. These results indicate that afadin is highly expressed in the ectoderm-derived cells during embryogenesis and plays a key role in proper organization of AJs and tight junctions of the highly expressing cells, which is essential for proper tissue morphogenesis.

Key words: afadin • cadherin • ZO-1 • cell–cell junctions • embryogenesis

Cell adhesion plays essential roles in tissue morphogenesis, which occurs either in embryos or in tissues undergoing development in adult organisms (Edelman, 1986; Takeichi, 1988, 1991, 1993; Albelda and Buck, 1990; Edelman and Crossin, 1991; Buck, 1992; Gumbiner, 1996). The cell adhesion–dependent morphogenetic processes in embryos are characterized at various stages by formation of polarized epithelial structures with tightly adherent cell–cell junctions. During gastrulation, embryonic ectodermal cells undergo epithelial–mesenchymal transition and form the embryonic mesoderm and endoderm. These mesenchymal cells forming along the primitive streak lose cell–cell adhesion and migrate at the space beneath the embryonic ectoderm. Some of them are subsequently reorganized to the epithelial structures of the mesoderm such as somites. Thus, reorganization of epithelial structures is essential for coordinated progression of body plan placement and cell specification. However, regulatory mechanisms for this reorganization have not been fully understood. To understand this cell adhesion–dependent morphogenesis, it is important to understand the molecular basis of cell adhesion of epithelia in developing embryos.

In polarized epithelial cells, cell–cell adhesion forms a specialized membrane structure, comprised of tight junctions (zonula occludens), cell–cell adherens junctions (AJs)[1] (zonula adherens), and desmosomes, which is known as the junctional complex. These junctional structures are typically aligned from the apical side to the basal side, although desmosomes are independently distributed in

Address correspondence to Yoshimi Takai, Department of Molecular Biology and Biochemistry, Osaka University Graduate School of Medicine/Faculty of Medicine, 2-2 Yamada-oka, Suita, Osaka 565-0871, Japan. Tel.: 81-6-6879-3410. Fax: 81-6-6879-3419. E-mail: ytakai@molbio.med.osaka-u.ac.jp

1. *Abbreviations used in this paper:* aa, amino acid(s); AJ, adherens junction; CAM, cell adhesion molecule; EB, embryoid body; ES, embryonic stem; F-actin, actin filament; Flk1, fetal liver kinase 1; PDGFRα, PDGF receptor α; *T*, *Brachyury*.

other areas. At cell–cell AJs, classic cadherins interact with each other at the extracellular surface in a Ca^{2+}-dependent manner and with the actin cytoskeleton at the cytoplasmic region through the peripheral membrane proteins, including α-, β-, and γ-catenins, α-actinin, and vinculin (Takeichi, 1988, 1991; Ozawa et al., 1989; Geiger and Ginsberg, 1991; Nagafuchi et al., 1991; Tsukita et al., 1992). Of these peripheral membrane proteins, α-catenin, α-actinin, and vinculin are actin filament (F-actin)–binding proteins (Knudsen et al., 1995; Rimm et al., 1995; Weiss et al., 1998). At tight junctions, the claudin family members and occludin constitute tight junction strands (Furuse et al., 1993, 1998; Ando-Akatsuka et al., 1996). They interact with each other at the extracellular surface and with the actin cytoskeleton through peripheral membrane proteins, including ZO-1 (Itoh et al., 1993, 1997). Thus, many F-actin–binding proteins serve as linkers of the actin cytoskeleton to cell adhesion molecules (CAMs) such as cadherin, claudin, and occludin. Accumulating evidence suggests that cadherin exhibits different functional states of cell–cell adhesion and plays crucial roles in the reorganization of epithelial structures during tissue morphogenesis (Takeichi, 1988, 1991; Gumbiner, 1996), although the roles of claudin and occludin in these processes are poorly understood. Little is known, either, about the mechanism by which the F-actin–binding proteins regulate the functional states of CAMs.

We have recently identified a novel cell–cell adhesion system, which is colocalized with the cadherin–catenin system at cell–cell AJs in polarized epithelial cells, but is more highly concentrated there than the cadherin–catenin system (Mandai et al., 1997, 1999; Takahashi et al., 1999). This adhesion system is composed of nectin, afadin, and ponsin, and named NAP system. Nectin is an Ig-like homophilic CAM that is identical to the poliovirus receptor–related protein (Morrison and Racaniello, 1992; Eberlé et al., 1995; Lopez et al., 1995), and has recently been identified to be the alphaherpesvirus entry mediator (Geraghty et al., 1998; Warner et al., 1998). The cytoplasmic region of nectin interacts with the actin cytoskeleton through afadin, an F-actin–binding protein. Afadin has two splicing variants, l- and s-afadins. l-Afadin is ubiquitously expressed, whereas s-afadin is abundantly expressed in neural tissue. l-Afadin has one PDZ domain at the middle region, three proline-rich regions following the PDZ domain, and one F-actin–binding domain at the COOH-terminal region. s-Afadin has one PDZ domain but lacks the third proline-rich region and the F-actin–binding domain. s-Afadin is identical to AF-6, the gene of which is originally found to be fused to the *ALL-1* gene in acute leukemia (Prasad et al., 1993). Ponsin is an l-afadin–binding protein which binds to vinculin and provides a possible linkage of nectin–afadin to cadherin–catenin through vinculin (Mandai et al., 1999). It has recently been reported that AF-6 (s-afadin) interacts and clusters with the Eph receptor tyrosine kinases at specialized sites of cell–cell contact in brain (Hock et al., 1998; Buchert et al., 1999). However, the biological functions of the NAP system remain to be established. To address this issue, here we generated afadin$^{-/-}$ mice and embryonic stem (ES) cells and characterized them.

Materials and Methods

Cloning of the Mouse Afadin Gene

A mouse brain cDNA library (Stratagene) was screened with a probe that was derived from the rat l-afadin cDNA (Mandai et al., 1997). 32 positive clones were subcloned into the pBluescript II vector and sequenced. A cDNA fragment containing the NH_2-terminal open reading frame of the mouse afadin cDNA (sequence data available from EMBL/GenBank/DDBJ under accession no. AF172447) was used to isolate genomic clones from a 129SVJ mouse genomic DNA library (Stratagene). Overlapping genomic clones were obtained and mapped with respect to the mouse afadin cDNA sequence.

Construction of the Afadin Gene Targeting Vector

A SacI-SphI genomic fragment (4.6 kb) 5′ to the afadin exon 2 encoding amino acids (aa) 36–100 was blunt-ended and inserted into the SmaI site of pBluescript neo/DT-A, which contained neomycin-resistance and diphtheria toxin A genes under the control of the MC1 promoter (Thomas and Capecchi, 1987; Yagi et al., 1990). The XbaI genomic fragment (5.3 kb) 3′ to exon 2 was then inserted into the EcoRV site of pBluescript neo/DT-A containing the 5′ genomic fragment. The ~1.0 kb SphI-XbaI fragment was targeted for disruption and replaced by the neomycin-resistant gene cassette (see Fig. 2). This fragment began at the SphI site within exon 2 and ended in the following intron, and contained the coding sequence of aa 85–100. In the targeting vector, a stop codon resided 36 bp 3′ from the encoded aa 84. For Southern blot analysis, a 0.9-kb SacI-HindIII fragment and a 1.0-kb XbaI fragment were used as 5′ and 3′ probes, respectively.

Selection of ES Cells and Generation of Afadin$^{-/-}$ Mice

129/Sv RW4 ES cells (Genome Systems Inc.) were cultured on STO feeder cells in high-glucose DME supplemented with 20% FCS, 0.1 mM 2-mercaptoethanol (Sigma Chemical Co.), 1,000 U/ml leukemia inhibitory factor (Amrad Co.), 0.1 mM nonessential aa (GIBCO BRL), 3 mM adenosine, 3 mM cytosine, 3 mM guanosine, 3 mM uridine, and 1 mM thymidine (Sigma Chemical Co.) (Robertson, 1987). The targeting vector (50 μg) was linearized by NotI digestion and electroporated into ES cells using an Electro Cell Manipulator 600 (BTX) set at 270 V and 500 μF (Koera et al., 1997). ES cells were plated onto G418-resistant STO feeder cells in normal growth medium for 48 h, followed by selection with 175 μg/ml G418. G418-resistant STO feeder cells were prepared as described (Rudnicki et al., 1992). After 7–10 d, G418-resistant colonies were picked up and their DNAs were isolated for Southern blot analysis (Sambrook et al., 1989). The colonies were screened by cleaving genomic DNA (15 μg) with HindIII and probing the Southern blot with the 5′ probe (see Fig. 2). The HindIII-digested genomic DNA was also similarly analyzed with the 3′ probe. Among the 120 G418-resistant ES clones, 14 clones underwent homologous recombination, which was confirmed by Southern blot analysis.

Three different ES clones with the targeted mutation of the afadin gene were used to generate chimeric mice by injection of C57BL/6 blastocysts with 10–20 ES cells (Bradley, 1987). The blastocysts were implanted into pseudopregnant MCH foster mothers. Chimeric mice were mated with BDF1 mice. Offsprings with agouti coat color were tested for the presence of the targeted afadin allele by Southern blot analysis. Heterozygous mice were interbred, and the resulting mice were genotyped.

DNA Isolation and Genotyping

Genomic DNA from ES cells was prepared as described (Robertson, 1987) and analyzed by Southern blot analysis as described above. The mice were genotyped by Southern blot analysis and/or PCR. Two sets of primers were used in the PCR reactions. One set of primers corresponded to the neomycin-resistance gene: 5′-GGGCGCCCGGTTCTTTTTGTC-3′ and 5′-GCCATGATGGATACTTTCTCG-3′. The other set of primers corresponded to exon 2 of the afadin gene: 5′-TTCTAGGATTTG-GAGTTTCAT-3′ and 5′-GGTCAGGACACAGTCTTCACT-3′ (see Fig. 2). Tail or yolk sac DNA was used for the PCR reactions (Hanley and Merlie, 1991).

Generation of Afadin$^{-/-}$ ES Cells

In the targeting vector for generation of afadin$^{+/-}$ ES cells, the G418-resistance gene was replaced by the puromycin-resistance gene (Tucker et

al., 1997). The resulting targeting vector was linearized by NotI digestion and electroporated into afadin$^{+/-}$ ES cells as described above. ES cells were then subjected to selection with 1.0 μg/ml puromycin (Sigma Chemical Co.) and analyzed by Southern blotting as described above. Among the 120 puromycin-resistant ES clones, 9 clones underwent homologous recombination, which was confirmed by Southern blot analysis. They were further analyzed by reverse transcription PCR using one set of primers corresponding to aa 187–316 of mouse afadin: 5′-CTCAAGGGGATGACAGTGAG-3′ and 5′-TCCTTAGCACCTCTCTCATC-3′.

Embryoid Body Formation

ES cells (6×10^6) were cultured without feeder cells on gelatin-coated 10-cm dishes for 3 d in the normal growth medium described above. Embryoid body (EB) formation was initiated by hanging drops of 1,000 cells in 20 μl of DME-supplemented 10% FCS in the absence of leukemia inhibitory factor (Robertson, 1987; Rudnicki and McBurney, 1987). After 2 d, formed EBs were transferred to 10-cm bacteriological dishes and allowed to grow in suspension culture in DME supplemented with 10% FCS. The media were changed every other day.

Antibodies

Rabbit polyclonal and mouse monoclonal anti–l-afadin (rat, aa 1814–1829) antibodies were prepared as described (Mandai et al., 1997; Sakisaka et al., 1999). A rabbit polyclonal antibody recognizing both l- and s-afadins (rat, aa 577–592) was prepared as described (Mandai et al., 1997). A mouse mAb recognizing both l- and s-afadins (human, aa 1091–1233) was purchased from Transduction Laboratories. Mouse anti–ZO-1 and antioccludin mAbs were kindly supplied by Drs. Sh. Tsukita, M. Itoh, and M. Furuse (Kyoto University, Kyoto, Japan). Mouse and rat (ECCD2) anti–E-cadherin mAbs were purchased from Transduction Laboratories and Takara Shuzo, Co., Ltd., respectively. Mouse antivinculin and anti–β-catenin mAbs were purchased from Sigma Chemical Co. and Zymed Laboratories Inc., respectively. Rat anti-PDGF receptor α (PDGFRα) and anti-fetal liver kinase 1 (Flk1) mAbs were prepared as described (Takakura et al., 1996; Kataoka et al., 1997).

Immunofluorescence Microscopy

Embryos dissected from their deciduae were fixed with 2% paraformaldehyde in PBS for 1 h, followed by extensive washing with PBS. The embryos were then suspended in 20% sucrose for 4 h, replaced with a solution (1:1 of 20% sucrose/OCT compound; Sakura Finetechnical Co., Ltd.), frozen in OCT compound, and sectioned on a cryostat at a thickness of 10 μm. Sections were mounted on glass slides, air-dried, and blocked in PSS (5% skim milk and 0.005% saponin in 0.1 M phosphate buffer, pH 7.5). The samples were then incubated with primary antibodies in PSS at 4°C overnight. They were washed with PSS and then incubated with secondary antibodies in PSS at 4°C for 2 h. After being washed with PSS, the samples were embedded and viewed with a confocal imaging system (MRC-1024; BioRad). EBs were also similarly fixed, frozen in OCT compound, and sectioned. Alternatively, EBs were directly frozen in OCT compound and sectioned on the cryostat. Sections were mounted on glass slides, air-dried, fixed with 95% ethanol at 4°C for 30 min, and then fixed with 100% acetone at room temperature for 1 min. They were processed as described above.

Whole-Mount Immunohistochemistry, Histological Analysis, and Whole-Mount In Situ Hybridization

Whole-mount immunohistostaining was performed as described (Takakura et al., 1997) with slight modifications. In brief, embryos dissected from their deciduae were washed with 0.1 M phosphate buffer and fixed with 2% paraformaldehyde in PBS at 4°C for 2 h to overnight according to the size of samples. The fixed samples were then bleached in a solution (methanol/30% H_2O_2 of 4:1). For staining, the rehydrated samples were first blocked in PBSMT (1% skim milk and 0.2% Triton X-100 in PBS), incubated with the anti–l-afadin polyclonal antibody in PBSMT at 4°C overnight, and washed extensively with PBSMT. The sample was then incubated with an HRP-conjugated antibody at 4°C overnight. After extensive washing, the samples were soaked in a solution of metal-enhanced DAB substrate kit (Pierce). The enzymatic reaction was allowed to proceed until the desired color intensity was reached, and the samples were washed with PBST. Staining with hematoxylin and eosin was performed as described (Kaufman, 1995). In brief, embryos dissected their deciduae and EBs were fixed with 2% paraformaldehyde in PBS at 4°C overnight, washed with PBS at 4°C overnight, dehydrated in graded alcohols, embedded in paraffin, sectioned at 3 μm, and stained with hematoxylin and eosin. Whole-mount in situ hybridization with the antisense RNA of *Brachyury* (*T*) as a probe was performed as described (Herrmann, 1991; Wilkinson, 1992) with slight modifications. In brief, the RNA probe was labeled with digoxigenin-UTP by RNA in vitro transcription according to the manufacturer's protocols (Boehringer Mannheim). The cDNA of *T* was kindly supplied by Dr. S. Takada (Kyoto University, Kyoto, Japan). The samples were incubated with an antidigoxigenin antibody conjugated to alkaline phosphatase, and the color was developed in NBT/BCIP solution (Boehringer Mannheim). The samples were frozen in OCT compound, sectioned as described above, and counterstained with neutral red.

Other Procedures

Protein concentrations were determined with BSA as a reference protein (Bradford, 1976). SDS-PAGE was done as described (Laemmli, 1970).

Results

Expression and Localization of l-Afadin during Early Embryogenesis

We first examined expression and localization of l-afadin during mouse early embryogenesis. At embryonic day 6.5 (E6.5), embryos developed to egg cylinders containing embryonic and extraembryonic regions and proamniotic cavities. The embryonic ectoderm was composed of high columnar epithelial cells surrounded by the visceral endoderm. Yolk sac and ectoplacental cone were clearly observed in this stage. Immunofluorescence microscopy of E6.5 embryos revealed that l-afadin was localized at the most apical regions of cell–cell adhesion sites, called the junctional complex regions, of the entire embryonic ectoderm, whereas the signals of F-actin were observed along the entire cell surface (Fig. 1 Aa and Ab). l-Afadin was hardly detected in the extraembryonic regions such as the visceral endoderm. At E7.0, embryos underwent primitive streak formation and mesoderm generation. Gastrulation began by the recruitment of embryonic ectodermal cells to the primitive streak, followed by exfoliation of cells from the primitive streak. Whole-mount immunohistochemistry revealed marked expression of l-afadin in the primitive streak and the migrating paraxial mesoderm (Fig. 1 B). At E7.5, l-afadin was highly concentrated at the junctional complex regions in the primitive streak region (neuroepithelium) and the neural fold/groove region, but it was hardly detected in other areas of the ectoderm (Fig. 1, Ca–Ce). It remains to be clarified whether l-afadin is downregulated or whether the proportion of ectodermal cells with low expression of l-afadin increases. By E8.5, normal embryos completed gastrulation and began organogenesis. The primitive streak regressed and newly organized tissues developed. High expression of l-afadin was detected in the tail bud, somites, and the paraxial mesoderm, which is being reorganized to form somites, neural tube, and intraembryonic coelomic cavity/pericardio-peritoneal canal that gives rise to pleura and pericardium (Fig. 1 Da). l-Afadin was highly concentrated at the junctional complex regions in neural tube, somites, and pericardio-peritoneal canal (Fig. 1, Db–Df). These results indicate that l-afadin is highly expressed in a restricted set of epithelial structures and highly concentrated at their junctional complex regions.

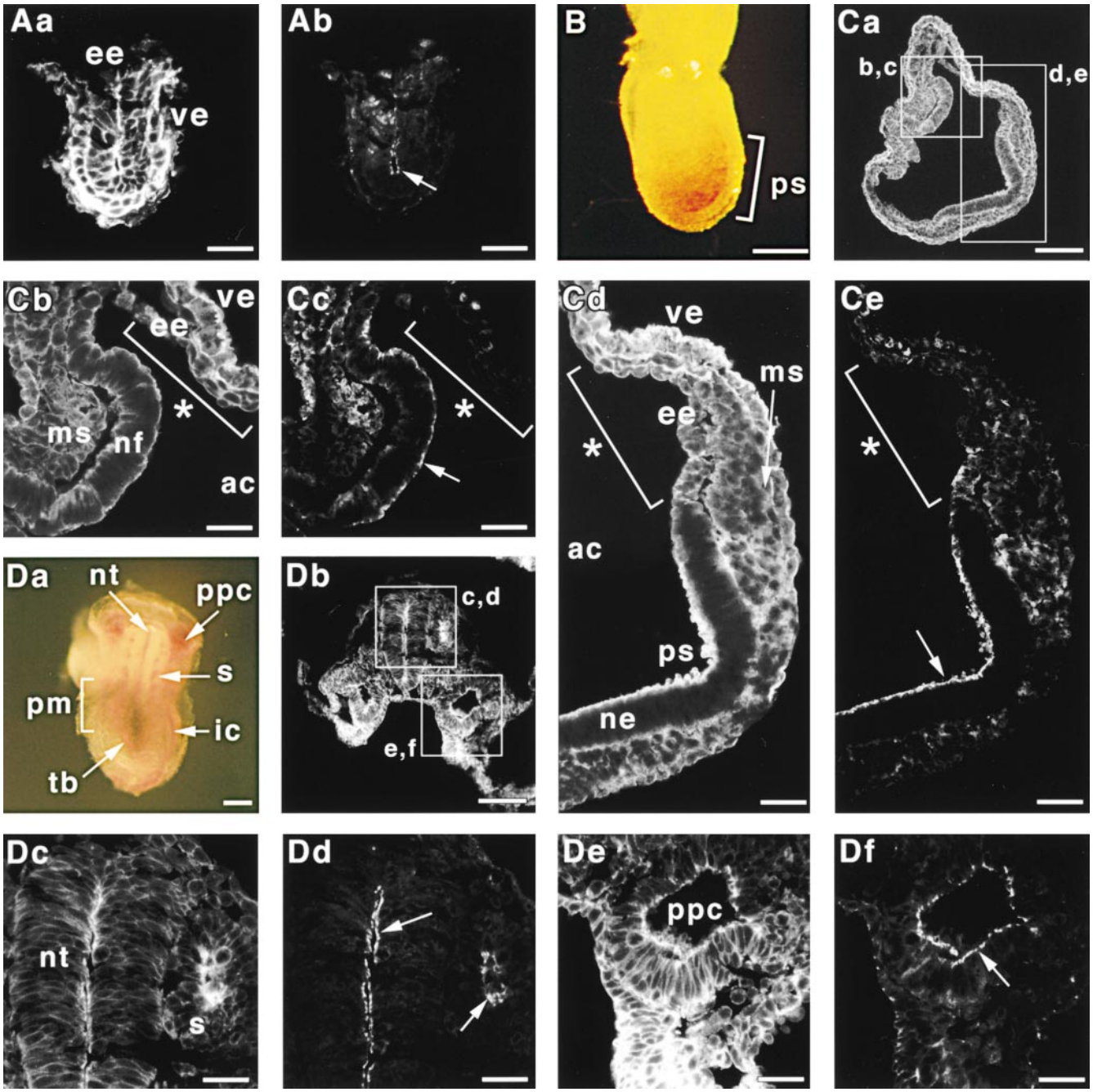

Figure 1. Expression and localization of l-afadin during early embryogenesis. Embryos at various stages were subjected to immunofluorescence microscopy and/or whole-mount immunohistochemistry. (A) Immunofluorescence microscopy of E6.5 embryos (transverse section). The samples were doubly stained with rhodamine-phalloidin and the polyclonal anti–l-afadin antibody. (Aa) F-actin; (Ab) l-afadin. (B) Whole-mount immunohistochemistry of E7.0 embryos (lateral view). The samples were stained with the polyclonal anti–l-afadin antibody. (C) Immunofluorescence microscopy of E7.5 embryos (transverse section). The samples were doubly stained with rhodamine-phalloidin and the polyclonal anti–l-afadin antibody. (Ca, Cb, and Cd) F-actin; (Cc and Ce) l-afadin; (Cb and Cc) double staining image with a high magnification of the indicated box b,c in Ca; and (Cd and Ce) double staining image with a high magnification of the indicated box d,e in Ca. (D) Whole-mount immunohistochemistry and immunofluorescence microscopy of E8.5 embryos. The samples were stained with the polyclonal anti–l-afadin antibody for whole-mount immunohistochemistry or with rhodamine-phalloidin and the anti–l-afadin antibody for immunofluorescence microscopy. (Da) Whole-mount immunohistochemistry (ventral view); (Db–Df) immunofluorescence microscopy (transverse section); (Db, Dc, and De) F-actin; (Dd and Df) l-afadin; (Dc and Dd) double staining image with a high magnification of the indicated box c,d in Db; and (De and Df) double staining image with a high magnification of the indicated box e,f in Db. Arrows indicate junctional complex regions. Asterisks indicate l-afadin–negative ectoderm. ee, embryonic ectoderm; ve, visceral endoderm; ps, primitive streak; ms, mesoderm; nf, neural fold; ac, amniotic cavity; ne, neuroepithelium; nt, neural tube; pm, paraxial mesoderm; tb, tail bud; ppc, pericardio-peritoneal canal; s, somite; ic, intraembryonic coelomic cavity. Bars, 30 μm (Aa, Ab, Cb–Ce, and Dc–Df); 100 μm (B, Ca, and Db); and 150 μm (Da).

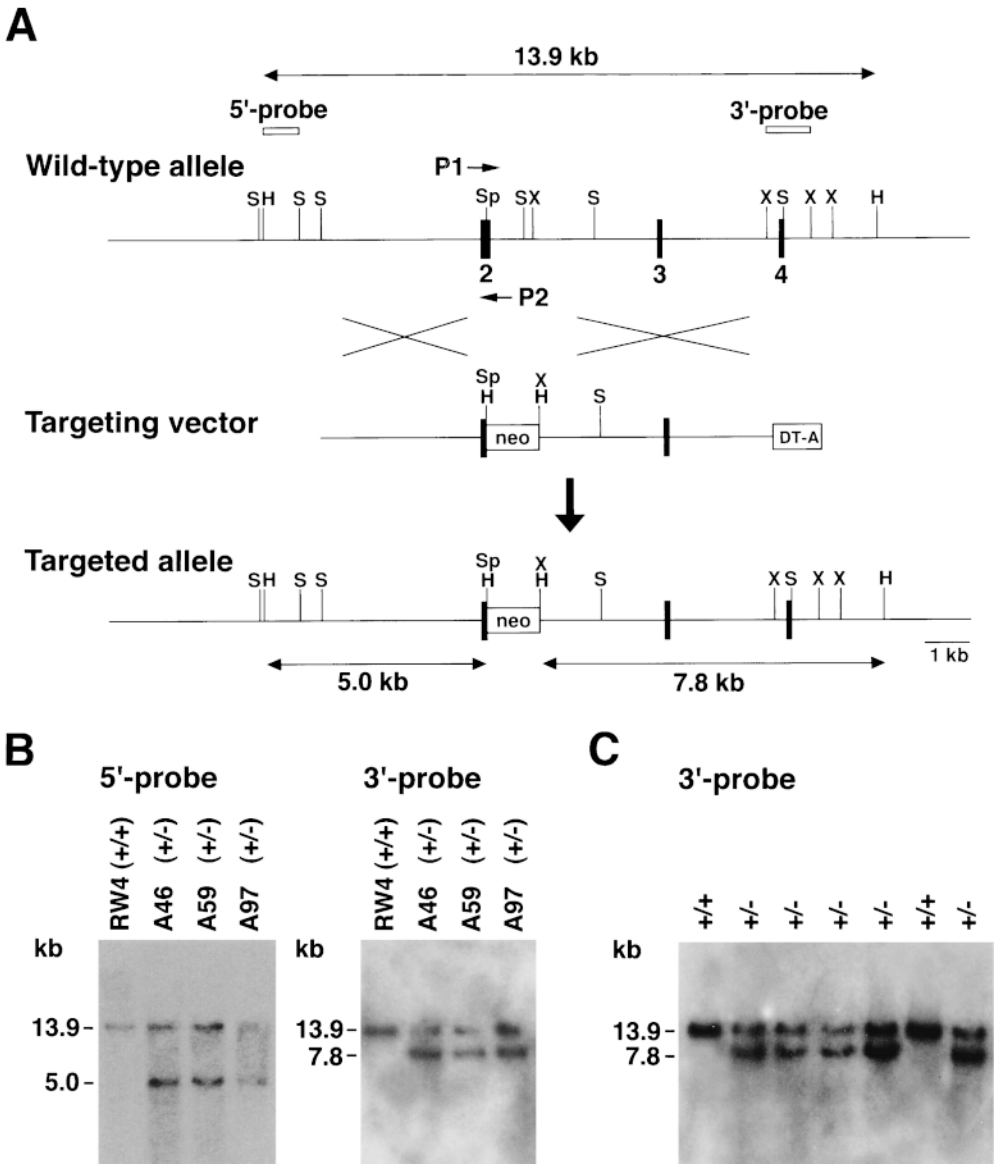

Figure 2. Targeted disruption of the afadin gene. (A) Restriction maps of the wild-type allele, the targeting vector, and the targeted allele of the afadin gene. Filled boxes, exons. S, SacI; H, HindIII; Sp, SphI; X, XbaI; P1, PCR primer, 5′-TTCTAGGATTTGGAGTTTCAT-3′; and P2, PCR primer, 5′-GGTCAGGACACAGTCTTCACT-3′. (B) Southern blot analysis of ES clones. HindIII-digested DNAs derived from ES cells were hybridized with the 5′ or 3′ probe. (C) Southern blot analysis of mice. The afadin$^{+/-}$ mice were intercrossed. HindIII-digested DNAs derived from tails of the progeny were hybridized with the the 3′ probe. +/+, wild type; and +/−, heterozygous mutant.

Targeting of the Afadin Locus

To determine the function of l-afadin in these epithelial structures, the mouse afadin gene was disrupted by homologous recombination. A targeting vector was designed so as to delete the exon 2 (Fig. 2 A). The linearized targeting vector was introduced into ES cells and subjected to selection using G418. To screen for homologous recombination events, genomic DNAs from G418-resistant clones were subjected to Southern blot analysis with a 5′ probe. The wild-type afadin allele displayed a 13.9-kb band on Southern blotting of HindIII-digested DNA, whereas the disrupted locus showed a 5.0-kb band (Fig. 2 B). Corrected targeting was confirmed by Southern blot analysis with a 3′ probe. The wild-type afadin allele displayed a 13.9-kb band, whereas the disrupted locus showed a 7.8-kb band. Three different ES clones (A46, A59, and A97) with the targeted allele were separately injected into host blastocysts, and the blastocysts were transferred to the uteri of pseudopregnant female mice. Germline transmission of the targeted allele was achieved with all ES clones. Inheritance of the targeted allele was determined by Southern blot analysis of the genomic DNA isolated from tail biopsies (Fig. 2 C). The heterozygous (afadin$^{+/-}$) mice appeared normal compared with the wild-type littermates. The afadin$^{+/-}$ mice were intercrossed and genotypes of the progeny were determined by Southern blot or PCR analysis using tail DNAs (Fig. 2 C). No homozygous (afadin$^{-/-}$) mice were detected among 82 progeny analyzed. These results indicate that deficiency of afadin causes embryonic lethality.

Developmental Defects of Afadin$^{-/-}$ Mice during Early Embryogenesis

Embryos were isolated at various stages of gestation and their genotypes were determined (Table I). Distribution of each genotype examined at E7.5–E9.5 followed the Mendelian law, whereas no homozygous embryos were detected from E10.5. At E6.5, gross morphological analysis

Table I. Genotypes of Progeny from Intercrosses of Afadin Heterozygous Mice

Stage	Total	Normal		Abnormal
		Wild-type	Afadin (+/−)	Afadin (−/−)
E7.5	100	23	58	19
E8.5	147	46	70	31
E9.5	22	8	8	6
Newborn	82	32	50	0

The mice were genotyped by Southern blot and/or PCR analysis using yolk sac or tail DNA.

did not distinguish the homozygous embryos from the wild-type and heterozygous littermates (data not shown), indicating that implantation and egg cylinder formation occur normally in the absence of afadin. To examine the presence of residual maternal afadin, which may affect implantation and egg cylinder formation in the homozygous embryos, preimplantation embryos at E3.5 (early blastocysts) were cultured and their levels of l-afadin were determined by immunofluorescence microscopy. Of 20 embryos examined, 16 showed weak but significant staining, whereas the remaining did not show any signal (data not shown). It is most likely that the latter embryos are homozygous and that there is no residual maternal afadin in the homozygous embryos. In contrast to embryos at E6.5, it was easy to distinguish the homozygous embryos from the wild-type and heterozygous littermates in embryos at E7.5–E9.5. Compared with wild-type embryos, the architecture of the homozygous embryos was apparently distorted and reduced in size (Fig. 3, Aa–Ac). Of note, however, is that their extraembryonic regions, including ectoplacental cone and yolk sac, developed normally, indicating that the anomalies are basically restricted to embryos proper. Whereas the anterior–posterior distinction could easily be made by gross appearance, and some vascular system and blood were detectable, the homozygous embryos were always flat and short, and no landmark tissues such as heart developed at this stage. The anomalies specific for these embryos proper in afadin$^{-/-}$ embryos are consistent with the expression patterns of l-afadin.

Disorganized Ectoderm in Afadin$^{-/-}$ Embryos during Gastrulation

In wild-type embryos at E7.5, delamination of mesodermal cells from the primitive streak was undertaken in a strictly polarized manner, thereby recruiting mesodermal cells into the space between the embryonic ectoderm and the visceral endoderm (Fig. 3 Ba). Of importance is that the integrity of epithelial structures of the ectoderm, including the primitive streak and neural groove, is maintained even under the stimulation to induce delamination. In afadin$^{-/-}$ embryos at E7.5, generation of mesodermal cells at this space did occur, indicating that mesoderm induction itself occurs normally (Fig. 3, Bb–Be). However, these mutant embryos had the wider space between the ectoderm and the endoderm, where more mesodermal cells were observed compared with wild-type embryos. Ectodermal cells of afadin$^{-/-}$ embryos appeared flat or cuboid, and their polarized epithelial structures appeared to be entirely impaired (Fig. 3, Bb–Be). At the region corresponding to neural fold/groove (from the anterior region to the distal region), the ectoderm became multilayered and appeared as a cell mass (Fig. 3, Bb–Be). At the posterior region corresponding to the primitive streak, the ectoderm was invaginated toward the amniotic side (Fig. 3, Bc and Be; see also Fig. 4 Bc, and Fig. 5, Ca, Cc, Ga, and Gc). The invaginated ectoderm often ran along with the ectoderm of the lateral region, resulting in the appearance of two layers. The space between the two layers corresponded to the amniotic cavity, which was compressed to an inverted U-shape. Cells were detected at the space surrounded by the invaginated ectoderm. Furthermore, in afadin$^{-/-}$ embryos, amniotic and exocoelomic cavities did not develop normally and formation of allantois was not observed (Fig. 3 Be). In contrast to the severe defects of the embryonic ectoderm, a single-layered epithelial structure in the endoderm remained intact (Fig. 3, Bb–Be). Hence, all of these phenotypes may be an outcome of abnormal progression of amniotic and chorionic membrane formation from the most proximal region of the primitive streak. In wild-type embryos at E8.5, tissues with epithelial structures, such as neural groove, intraembryonic coelomic cavity, and somites, were clearly evident (Fig. 3 Ca). In afadin$^{-/-}$ embryos, consistent with histological findings showing generation of mesodermal cells, gross appearance showed that somite-like blocks and some vascular structures were detected (data not shown), although no epithelial structure of somites was established (Fig. 3 Cb). Formation of neither neural tube nor heart was observed.

To further dissect the developmental defects of afadin$^{-/-}$ embryos, we next investigated expression of E-cadherin and mesoderm markers, including *T*, PDGFRα, and Flk1 at E7.5. Consistent with an earlier observation (Wilkinson et al., 1990), *T* was highly expressed in the primitive streak and its nascent mesoderm in wild-type embryos (Fig. 4, Aa and Ab). In afadin$^{-/-}$ embryos, the *T*-positive area appeared to be divided into two portions that corresponded to the most posterior regions of the two-layered ectoderm (Fig. 4, Ba–Bd). At the primitive streak stage, E-cadherin is expressed in the entire embryonic ectoderm (Takeichi, 1988). PDGFRα is expressed in the paraxial mesoderm (Takakura et al., 1997), and Flk1 is expressed in the proximal lateral mesoderm and the extraembryonic mesoderm (Kataoka et al., 1997). After completion of exfoliation from the primitive streak, E-cadherin was downregulated, and PDGFRα and Flk1 were expressed in the mesodermal cells (Fig. 5, Aa–Ac and Ea–Ec). In afadin$^{-/-}$ embryos, E-cadherin–negative and PDGFRα-positive cells were detected at the space between the ectoderm and the endoderm (Fig. 5, Ba–Bc, Ca–Cc, and Da–Dc). These cells corresponded to the mesodermal cells of the paraxial region. At the proximal region of the primitive streak, E-cadherin–positive cells were jammed at the space between the ectoderm and the endoderm (Fig. 5, Ba, Bc, Fa, and Fc; see also Fig. 6, Ca, Cc, Da, and Dc). The staining for E-cadherin clearly demonstrated that the E-cadherin–positive ectoderm was invaginated from the posterior region toward the amniotic side (Fig. 5, Ca and Cc). The most posterior region of the two-layered ectoderm corresponded to the area positive for *T* (Fig. 5, Ca and Cc; see also Fig. 4 Bc). E-cadherin–negative and PDGFRα-posi-

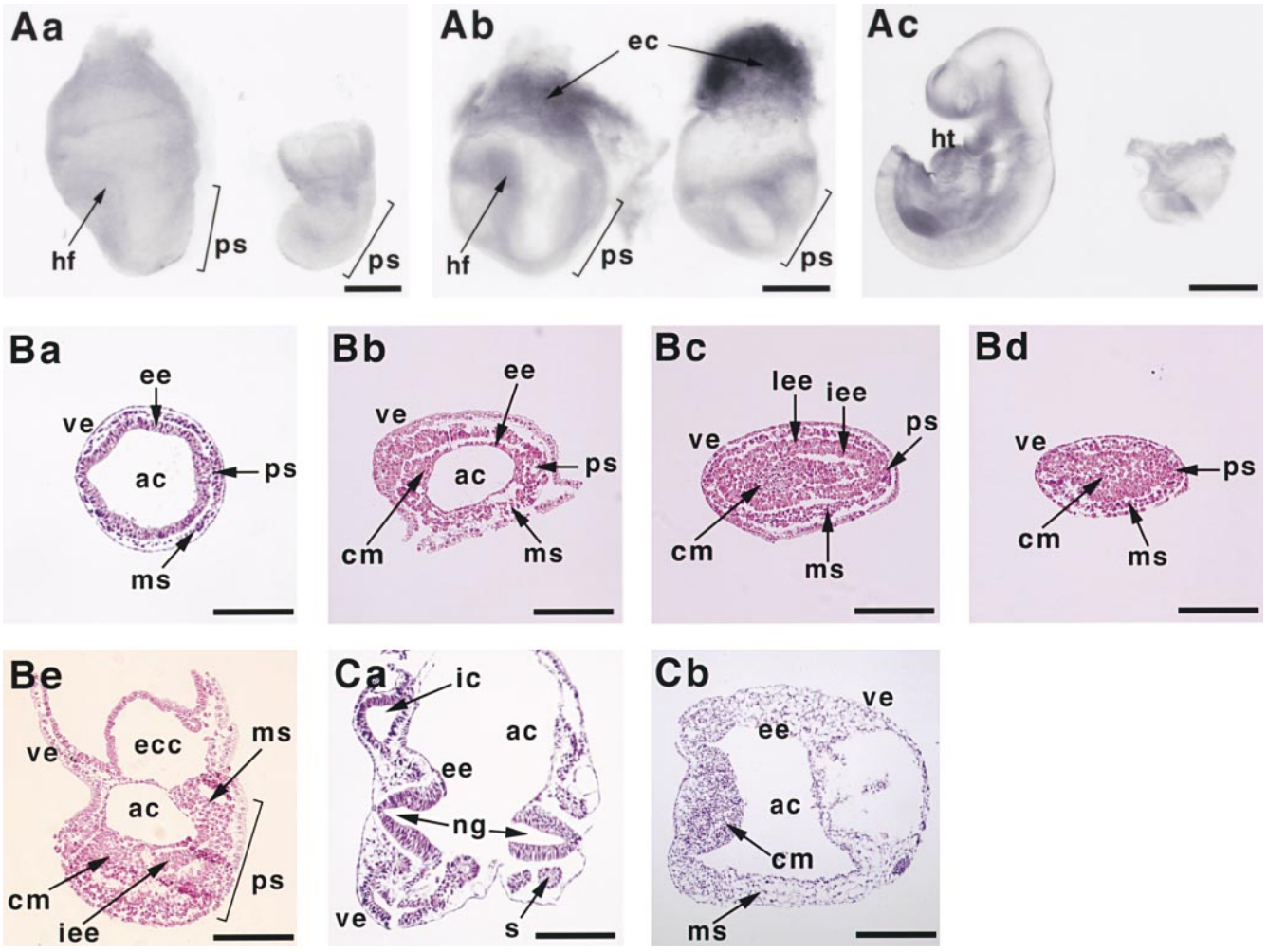

Figure 3. Developmental defects of afadin$^{-/-}$ embryos during early embryogenesis. (A) Gross appearance. (Aa) E7.5 embryos; (Ab) E8.5 embryos; and (Ac) E9.5 embryos: left, wild-type embryos; and right, afadin$^{-/-}$ embryos. (B) Histological analysis of E7.5 embryos. E7.5 embryos were subjected to staining with hematoxylin and eosin. (Ba) Wild-type embryos (transverse section); (Bb–Be) afadin$^{-/-}$ embryos; (Bb) transverse section of the proximal region; (Bc) transverse section of the middle region; (Bd) transverse section of the distal region; and (Be) sagittal section. (C) Histological analysis of E8.5 embryos. E8.5 embryos were subjected to staining with hematoxylin and eosin. (Ca) Wild-type embryos (transverse section); and (Cb) afadin$^{-/-}$ embryos (transverse section). hf, headfold; ps, primitive streak; ec, ectoplacental cone; ht, primitive heart; ee, embryonic ectoderm; ve, visceral endoderm; ac, amniotic cavity; ms, mesoderm; cm, cell mass; lee, lateral region of the embryonic ectoderm; iee, invaginated embryonic ectoderm; ecc, exocoelomic cavity; ic, intraembryonic coelomic cavity; ng, neural groove; and s, somite. Bars, 150 μm (Aa, Ba–Be, Ca, and Cb); 300 μm (Ab); and 350 μm (Ac).

tive cells were detected at the space surrounded by the invaginated ectoderm. These cells appeared to migrate from the primitive streak. At the regions corresponding to neural fold/groove (from the anterior region to the distal region), the multilayered cells were E-cadherin–positive (Fig. 5, Ba, Bc, Ca, Cc, Da, and Dc). At the distal region, some cells in the cell mass expressed not only E-cadherin but also PDGFRα (Fig. 5, Da–Dc). This cell mass was surrounded by a layer of the ectodermal cells that were E-cadherin–positive and PDGFRα-negative. Similar observations were obtained with the double staining for E-cadherin and Flk1, except that Flk1 was not expressed in the cell mass (Fig. 5, E–H). These observations strongly suggest that the major histological basis of the developmental defects of afadin$^{-/-}$ mice is disorganization of the embryonic ectoderm, and that distorted placement of various cell lineages is the secondary outcome of this disorganization.

Disorganized Cell–Cell Junctions of the Ectoderm in Afadin$^{-/-}$ Embryos

To investigate whether or not the apparatus for maintaining cell polarity is disturbed in the embryonic ectoderm, we examined the localization of E-cadherin and ZO-1 in afadin$^{-/-}$ embryos at E7.5. At the primitive streak region (neuroepithelium) and the neural fold/groove region in wild-type embryos, E-cadherin was concentrated at the junctional complex regions, although its signals were detected along the lateral membrane (Fig. 6, Aa, Ac, Ba and Bc). ZO-1 was exclusively localized at the junctional complex regions of the embryonic ectoderm (Fig. 6, Ab, Ac,

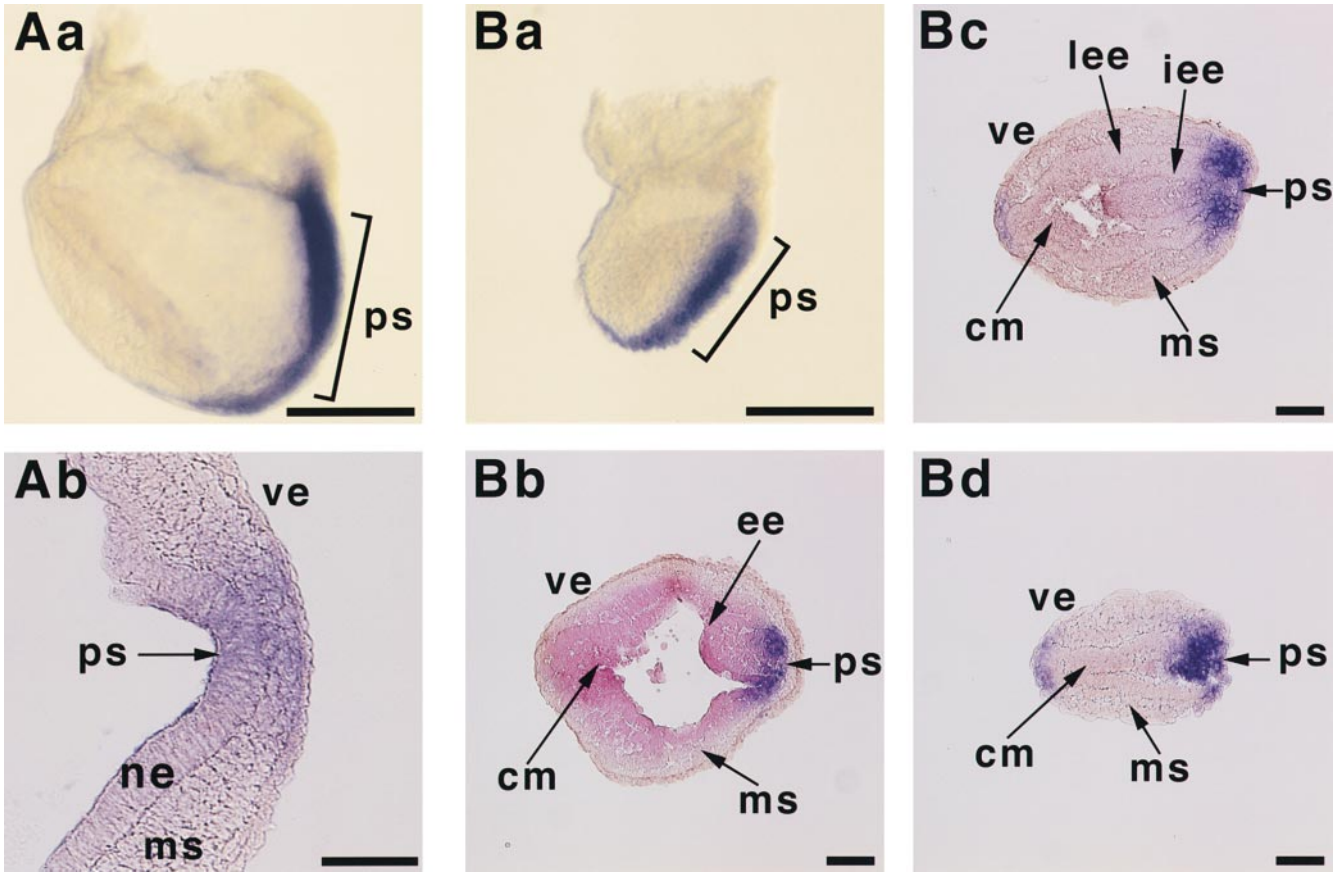

Figure 4. Abnormal primitive streak in afadin$^{-/-}$ embryos. E7.5 embryos were subjected to whole-mount in situ hybridization with the digoxigenin-labeled antisense RNA of *T* as a probe, sectioned, and counterstained with neutral red. (A) Wild-type embryos. (Aa) Lateral view; and (Ab) transverse section. (B) Afadin$^{-/-}$ embryos. (Ba) Lateral view; (Bb) transverse section of the proximal region; (Bc) transverse section of the middle region; and (Bd) transverse section of the distal region. ps, primitive streak; ve, visceral endoderm; ne, neuroepithelium; ms, mesoderm; ee, embryonic ectoderm; cm, cell mass; lee, lateral region of the embryonic ectoderm; and iee, invaginated embryonic ectoderm. Bars, 150 μm (Aa and Ba); and 30 μm (Ab and Bb–Bd).

Bb, and Bc). At the primitive streak region in afadin$^{-/-}$ embryos, E-cadherin hardly showed such an organized concentration as observed in wild-type embryos (Fig. 6, Ca, Cc, Da, and Dc). In the cell mass from the anterior region to the distal region, E-cadherin was distributed diffusely over the entire cell surface (Fig. 6, Ca, Cc, Ea, Ec, Fa, and Fc). The localization of ZO-1 was also disturbed in afadin$^{-/-}$ embryos. At the primitive streak region, ZO-1 was mainly localized at the most apical regions, but the signals were also detected in the basal regions (Fig. 6, Cb, Cc, Db, and Dc). In the cell mass, ZO-1 showed dotty signals in a random manner (Fig. 6, Eb, Ec, Fb, and Fc). These results indicate that deficiency of afadin induces disorganization of cell–cell junctions of the embryonic ectoderm.

Demonstration of Ectoderm-specific Afadin Function in an In Vitro Model System

The results of afadin$^{-/-}$ embryos indicate the following: (a) afadin is not essential for processes earlier than egg cylinder formation; (b) afadin is not required for anterior–posterior body plan placement in egg cylinders; and (c) afadin is expressed specifically in the embryonic ectoderm, particularly the primitive streak region (neuroepithelium) and the neural fold/groove region, and plays an essential role in the junctional organization in the ectoderm during gastrulation.

To determine whether or not the defects in afadin$^{-/-}$ embryos can be reproduced in a simpler model system, we took advantage of EB formation of ES cells where development of two-layered epithelial structures and subsequent mesoderm induction from the inner layer are shown to be reproduced in vitro (Doetschman et al., 1985; Robertson, 1987; Rudnicki and McBurney, 1987). For this purpose, we first established an afadin$^{-/-}$ ES cell line by introducing another targeting vector harboring puromycin-resistant gene (Fig. 7 A). This targeting vector was introduced into afadin$^{+/-}$ ES cells (clone A46). ES cells were subjected to selection using puromycin. Southern blot analysis showed that three clones (B3, B8, and B103) resistant to puromycin underwent gene conversion, resulting in disruption of both alleles (Fig. 7 B). Western blot analysis using the anti–l-afadin (rat, aa 1814–1829) mAb and the mAb recognizing both l- and s-afadins (human, aa 1091–1233) revealed the loss of afadin in afadin$^{-/-}$ ES cells and EBs (Fig. 7 C). Similar results were obtained with

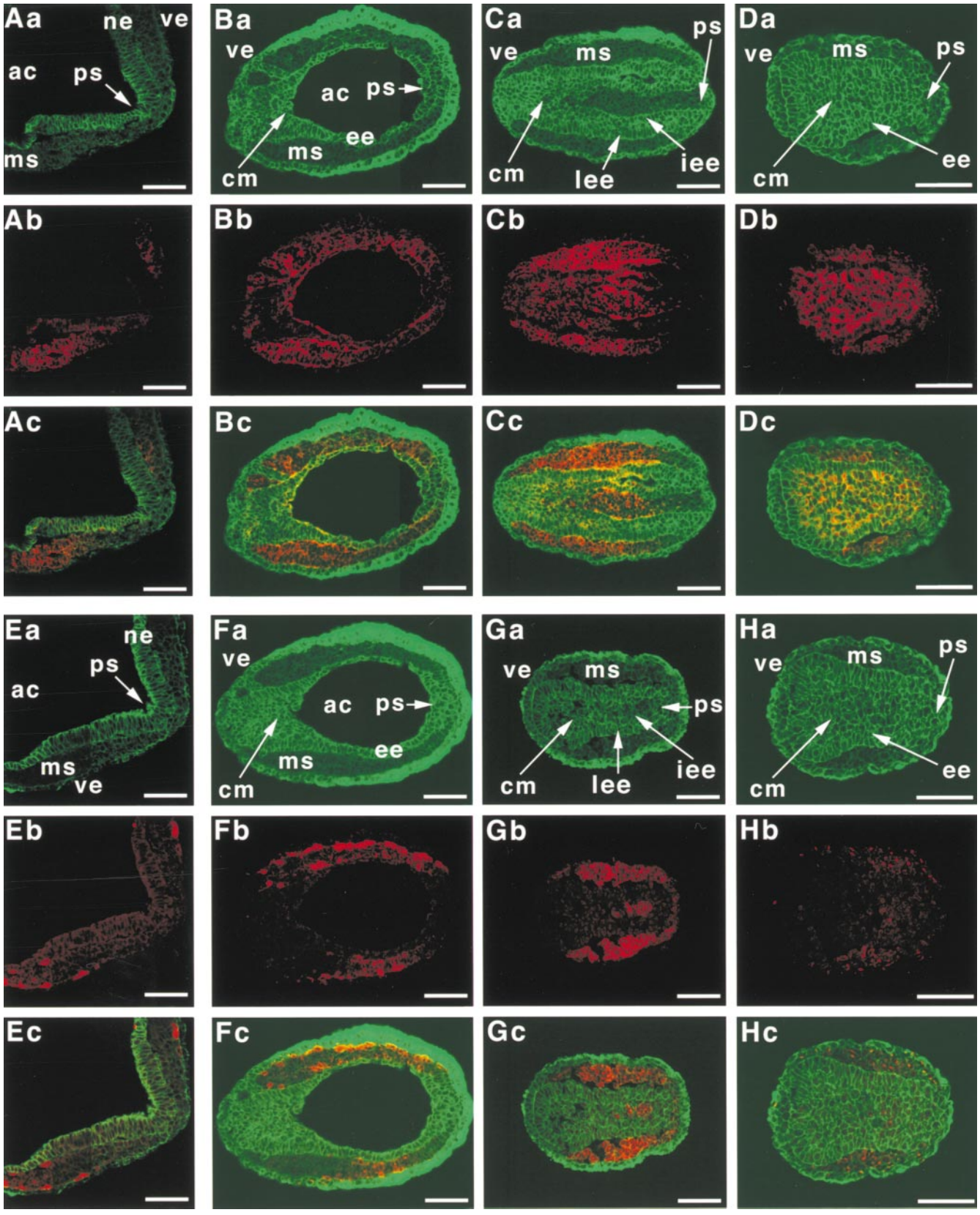

Figure 5. Disorganized ectoderm in afadin$^{-/-}$ embryos. Transverse sections of E7.5 embryos were doubly stained with the anti–E-cadherin antibody and the anti-PDGFRα or anti-Flk1 antibody for immunofluorescence microscopy. (A and E) Wild-type embryos; (B–D and F–H) afadin$^{-/-}$ embryos; (B and F) proximal region; (C and G) middle region; (D and H) distal region; (A–D) double staining with the anti–E-cadherin and anti-PDGFRα antibodies; (E–H) double staining with the anti–E-cadherin and anti-Flk1 antibodies. (Aa, Ba, Ca, Da, Ea, Fa, Ga, and Ha) E-cadherin; (Ab, Bb, Cb, and Db) PDGFRα; (Eb, Fb, Gb, and Hb) Flk1; and (Ac, Bc, Cc, Dc, Ec, Fc, Gc, and Hc) merge. ac, amniotic cavity; ms, mesoderm; ne, neuroepithelium; ve, visceral endoderm; ps, primitive streak; ee, embryonic ectoderm; cm, cell mass; lee, lateral region of the embryonic ectoderm; iee, invaginated embryonic ectoderm. Bars, 60 μm.

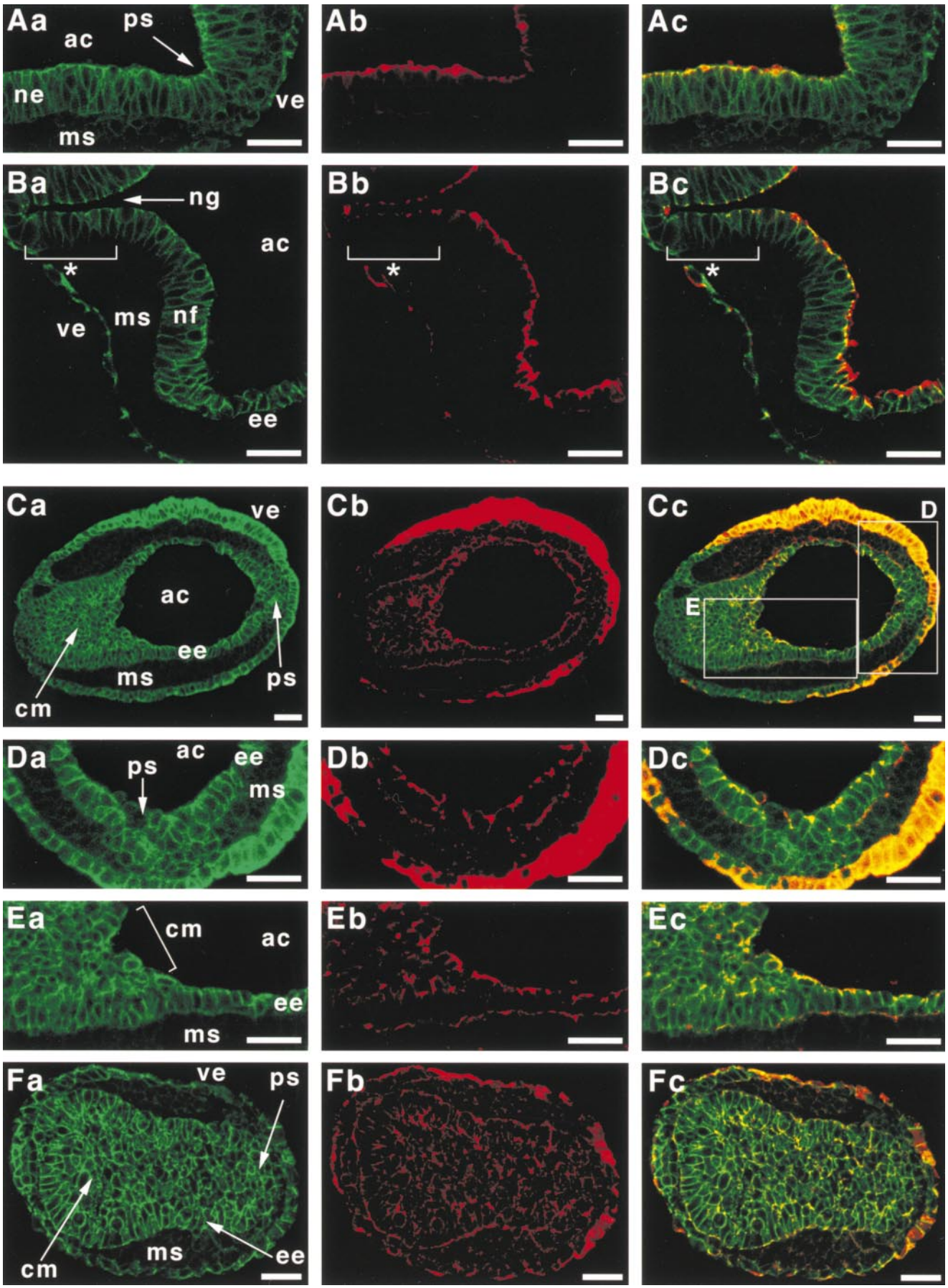

Figure 6. Disorganized cell–cell junctions of the embryonic ectoderm in afadin$^{-/-}$ embryos. Transverse sections of E7.5 embryos were doubly stained with the anti–E-cadherin and anti–ZO-1 antibodies. (A and B) Wild-type embryos; (C–F) afadin$^{-/-}$ embryos; (C) proxi-

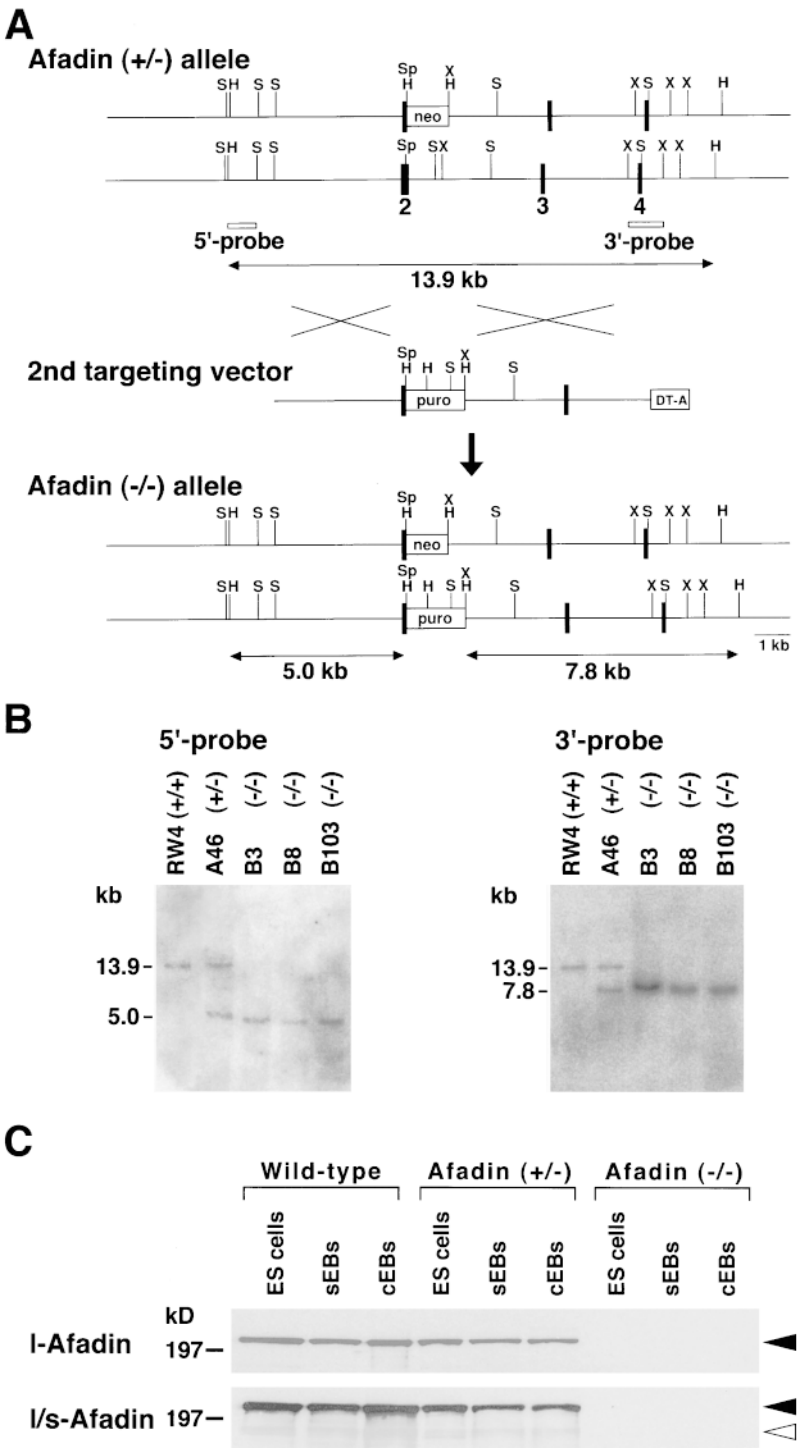

Figure 7. Generation of afadin$^{-/-}$ ES cells. (A) Restriction maps of the afadin$^{+/-}$ allele, the second targeting vector, and the afadin$^{-/-}$ allele of the afadin gene. Filled boxes, exons. S, SacI; H, HindIII; Sp, SphI; and X, XbaI. (B) Southern blot analysis. HindIII-digested DNAs derived from ES cells were hybridized with the 5′ or 3′ probe. (C) Western blot analysis. A cell lysate of ES cells, simple EBs, or cystic EBs (20 μg of protein each) was subjected to SDS-PAGE (8% polyacrylamide gel), followed by Western blot analysis using the anti–l-afadin mAb or the mAb recognizing both l- and s-afadins. sEBs, simple EBs. cEBs, cystic EBs. Black arrowheads indicate l-afadin and white arrowhead indicates s-afadin.

the polyclonal antibody recognizing both l- and s-afadins (rat, aa 577–592) (data not shown). Western blot analysis also revealed that l-afadin was a major expressed variant in wild-type ES cells and EBs, and that s-afadin was hardly detected (Fig. 7 C). Reverse transcription PCR analysis using the primer set corresponding to aa 188–316 of mouse afadin showed the loss of the afadin mRNA in afadin$^{-/-}$ ES cells (data not shown). The three independent clones

mal region; (D) high magnification of the indicated box D in Cc; (E) high magnification of the indicated box E in Cc; and (F) distal region. (Aa, Ba, Ca, Da, Ea, and Fa) E-cadherin; (Ab, Bb, Cb, Db, Eb, and Fb) ZO-1; and (Ac, Bc, Cc, Dc, Ec, and Fc) merge. Asterisks indicate a typical region where E-cadherin is concentrated at the junctional complex regions. ps, primitive streak; ac, amniotic cavity; ne, neuroepithelium; ms, mesoderm; ve, visceral endoderm; ng, neural groove; nf, neural fold; ee, embryonic ectoderm; and cm, cell mass. Bars, 30 μm.

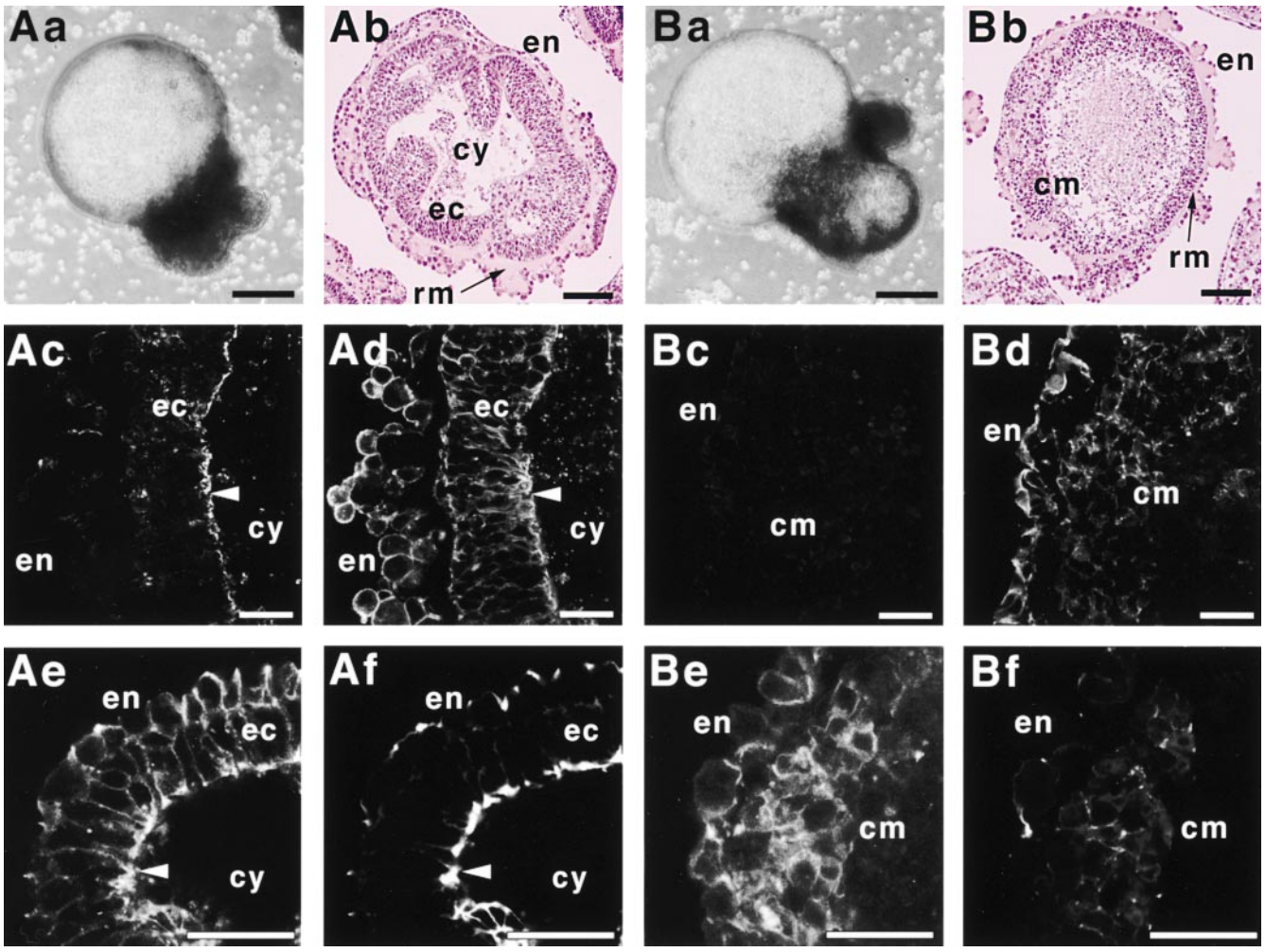

Figure 8. Disorganized ectoderm in cystic EBs derived from afadin$^{-/-}$ ES cells. Cystic EBs were subjected to histological analysis or immunofluorescence microscopy. For immunofluorescence microscopy, cystic EBs were doubly stained with rhodamine-phalloidin and the polyclonal anti–l-afadin antibody, or with the anti–E-cadherin and anti–ZO-1 antibodies. (A) Cystic EBs derived from wild-type ES cells; (B) cystic EBs derived from afadin$^{-/-}$ ES cells; (Aa and Ba) microscopic appearance; (Ab and Bb) staining with hematoxylin and eosin; (Ac, Ad, Bc, and Bd) double staining with rhodamine-phalloidin and the anti–l-afadin antibody; (Ac and Bc) l-afadin; (Ad and Bd) F-actin; (Ae, Af, Be, and Bf) double staining with the anti–E-cadherin and anti–ZO-1 antibodies; (Ae and Be) E-cadherin; and (Af and Bf) ZO-1. Arrowheads indicate junctional complex regions. en, endodermal layer; cy, cyst cavity; ec, ectodermal layer; rm, Reichert's membranes; and cm, cell mass. Bars, 150 μm (Aa and Ba); 100 μm (Ab and Bb); and 30 μm (Ac–Af and Bc–Bf).

of afadin$^{-/-}$ ES cells showed the same growth rate with undifferentiated morphology as wild-type ES cells did (data not shown). Since these clones showed the same phenotypes as far as examined, the data obtained from clone B3 were represented below.

When wild-type ES cells were subjected to suspension culture, cells aggregated to form EBs, some of which eventually develop to a two-layered cystic structure consisting of the outer endodermal layer and the inner high columnar ectodermal layer, although EBs with more complex structures with a large yolk sac–like cyst were often observed (Fig. 8, Aa and Ab). During earlier stages of EB formation, afadin$^{-/-}$ ES cells showed no significant difference (data not shown). Moreover, EBs with a large yolk sac–like cyst were often formed, suggesting that the endodermal components function normally (Fig. 8 Ba). On the other hand, in EBs with an amniotic cavity–like cyst, many necrotic cells were found in the cavity, while leaving the outer layer intact (Fig. 8 Bb). Generation of mesodermal cells at the space between the ectodermal and endodermal layers was observed, but the well-organized ectodermal layer did not develop. These results indicate that the ectoderm-specific defects of afadin$^{-/-}$ embryos may be reproduced in the in vitro EB model. Moreover, the presence of cellular components in the EB cavity may reflect the defects in the polarity of the ectodermal layer.

To investigate whether deficiency of afadin affects expression of other components of cell–cell junctions, we compared expression levels of E-cadherin, β-catenin, vinculin, ZO-1, and occludin, in wild-type and afadin$^{-/-}$ ES cells during EB formation. We could not detect any significant difference in their expression levels (data not shown).

Cytological Basis for the Defect of Afadin$^{-/-}$ EBs

EBs with an amniotic cavity–like cyst were selected and subjected to immunofluorescence microscopy using antibodies against various components of cell–cell junctions. Consistent with the results on embryos, cells in the ectodermal layer, but not in the outer endodermal layer of wild-type EBs expressed l-afadin (Fig. 8 Ac). However, unlike embryos with the high expression along the anterior–posterior axis, l-afadin was expressed ubiquitously in the ectodermal layer. l-Afadin was concentrated at the junctional complex regions where F-actin was concentrated, although diffuse distribution of F-actin along the entire cell surface was also observed (Fig. 8, Ac and Ad). In afadin$^{-/-}$ EBs, no afadin signal was observed (Fig. 8 Bc), indicating that the function of the gene is completely disrupted. Although no abnormality was found in the outer endodermal layer, formation of the organized junctional complex was severely inhibited in the ectodermal layer (Fig. 8, Bd–Bf). F-actin showed diffuse distribution along the entire cell surface without any concentration in the ectodermal layer (Fig. 8 Bd). Compared with the organized concentration of E-cadherin at the junctional complex regions in wild-type EBs (Fig. 8 Ae), E-cadherin was diffusely distributed over the ectodermal cell surface (Fig. 8 Be). Likewise, compared with the organized localization of ZO-1 in wild-type EBs (Fig. 8 Af), it was displayed as dotty signals in a random manner in the cell mass (Fig. 8 Bf).

Discussion

The first implication of this study is that l-afadin is expressed only in a restricted set of epithelial structures during early embryogenesis. This goes against the notion that l-afadin is a constitutive component of cadherin-based cell–cell AJs. In fact, high expression of l-afadin is observed in such regions as the primitive streak region (neuroepithelium), neural fold/groove, and somites, where dynamic tissue rearrangements are ready to occur. On the other hand, only a low level if any of l-afadin expression is detected in other epithelial structures such as the visceral endoderm, which may expand but take a simpler differentiation course. The essentially similar expression patterns are reproduced in an in vitro model system of EB formation, suggesting that its expression is coordinated to each cell specification program. Further studies are required to determine whether l-afadin is expressed inducibly in the regions where new tissues develop from epithelia through dynamic cell rearrangement.

In agreement with the expression patterns of l-afadin during gastrulation, afadin$^{-/-}$ embryos display major defects in the embryonic ectoderm. This indicates that no redundancy exists in the function of afadin during gastrulation. Delamination of mesodermal cells does occur. As the cells, which are observed at the space surrounded by the invaginated ectoderm as well as at the space between the ectoderm and the endoderm, are E-cadherin–negative and PDGFRα-positive, mesoderm differentiation can occur normally if placed in the correct environment. This is consistent with the fact that mesoderm-derived structures develop to some extent also in afadin$^{-/-}$ embryos. Thus, mesoderm differentiation per se is not affected by this mutation. The most remarkable phenotype is the invagination of the ectoderm to the amniotic side, which never occurs in normal embryogenesis. This invagination divides the primitive streak into two portions as examined by the staining for *T*. Furthermore, this mutation produces the cell mass in the region corresponding to neural fold/groove. Some cells in the cell mass express both E-cadherin and PDGFRα, but not Flk1. As such double positive cells are found in stripes of ectodermal cells at the edge of neural groove of prorhombomeres (Takakura et al., 1997), it is likely that the cell mass represents this subset of the ectoderm. While it is attractive to think that afadin also plays a direct role in organization of epithelial structures such as neural tube, somites, and intraembryonic coelomic cavity/pericardio-peritoneal canal where a high level of l-afadin expression is detected, disorganization of the ectoderm in afadin$^{-/-}$ embryos does not allow investigation of these processes.

The design of the targeting vector used in this study raises the possibility that the truncated afadin polypeptide (aa 1–84) is produced both in afadin$^{-/-}$ mice and ES cells and in afadin$^{+/-}$ mice and ES cells. It can not completely be neglected that the truncated afadin polypeptide may contribute to the phenotypes of afadin$^{-/-}$ mice and EBs shown here. However, this possibility is unlikely because any known, functional domain or motif is not included in this polypeptide, and afadin$^{+/-}$ mice and ES cells develop normally.

An issue here is closely related to the problem of cell biology, i.e., how epithelial cells maintain the structural integrity with polarity. Our results clearly indicate that structural integrity of epithelia such as the trophoectoderm and the visceral endoderm can be maintained in the absence of afadin. This is more clearly addressed in the development of afadin$^{-/-}$ EBs. Formation of yolk sac–like large cysts in some of afadin$^{-/-}$ EBs indicates that endodermal cells differentiate, proliferate, and maintain the integrity of epithelial structures, which are essential for transporting and sealing fluid in the cyst. Thus, at least during early embryogenesis, afadin plays a key role in actively rearranging epithelia of the embryonic ectoderm, such as the primitive streak and neural fold/groove. As the mesoderm can be produced in afadin$^{-/-}$ embryos, gastrulation itself appears to occur. Instead, we have highlighted processes during formation of the primitive streak and neural fold/groove. Under such a situation, active reorganization of epithelial structures is induced, but the structural integrity of epithelia should be maintained and its basic structures such as polarity have to be preserved, otherwise newly generated tissues cannot be organized. Afadin is indeed a key molecule for these processes.

Afadin is a linker of nectin, an Ig-like CAM, with the actin cytoskeleton (Takahashi et al., 1999). Ig-like CAMs are implicated in tissue morphogenesis, particularly cell migration (Edelman, 1986; Williams and Barclay, 1988; Buck, 1992; Walsh and Doherty, 1997). The result, that epithelial organization as defined by a correct distribution of ZO-1 in the ectoderm is disrupted completely in the absence of afadin, suggests that afadin regulates the functional state of nectin, thereby contributing to the basic organization of cell–cell junctions of the ectoderm. Although

further studies are necessary to establish the role of afadin in these processes, this study has highlighted not only the role of afadin but also the importance of epithelial organization of the embryonic ectoderm during gastrulation. Thus, we expect that further studies on the role of afadin and its associated molecules will open a new avenue bridging the border of cell biology and developmental biology.

We thank Drs. Sh. Tsukita, M. Itoh, and M. Furuse for supplying the anti–ZO-1 and antioccludin antibodies and for helpful discussion, and Dr. S. Takada for the cDNA of *Brachyury*. We are also grateful to Dr. M. Takeichi (Kyoto University, Kyoto, Japan) for helpful discussion.

Submitted: 11 June 1999
Revised: 30 July 1999
Accepted: 2 August 1999

References

Albelda, S.M., and C.A. Buck. 1990. Integrin and other cell adhesion molecules. *FASEB J.* 4:2868–2880.

Ando-Akatsuka, Y., M. Saitou, T. Hirase, M. Kishi, A. Sakakibara, M. Itoh, S. Yonemura, M. Furuse, and Sh. Tsukita. 1996. Interspecies diversity of the occludin sequence: cDNA cloning of human, mouse, dog, and rat-kangaroo homologues. *J. Cell Biol.* 133:43–47.

Bradford, M.M. 1976. A rapid and sensitive method for the quantitation of microgram quantities of protein utilizing the principle of protein-dye binding. *Anal. Biochem.* 72:248–254.

Bradley, A. 1987. Production and analysis of chimeric mice. *In* Teratocarcinomas and Embryonic Stem Cells: A Practical Approach. E.J. Robertson, editor. IRL Press, Oxford. 113–151.

Buchert, M., S. Scheider, V. Maskenaite, M.T. Adams, E. Canaani, T. Baechi, K. Moelling, and C.M. Hovens. 1999. The junction-associated protein AF-6 interacts and clusters with specific Eph receptor tyrosine kinases at specialized sites of cell–cell contact in the brain. *J. Cell Biol.* 144:361–371.

Buck, C.A. 1992. Immunoglobulin superfamily: structure, function and relationship to other receptor molecules. *Semin. Cell Biol.* 3:179–188.

Doetschman, T.C., H. Eistetter, M. Katz, W. Schmidt, and R. Kemler. 1985. The in vitro development of blastocyst-derived embryonic stem cell lines: formation of visceral yolk sac, blood islands and myocardium. *J. Embryol. Exp. Morphol.* 87:27–45.

Eberlé, F., P. Dubreuil, M.G. Mattei, E. Devilard, and M. Lopez. 1995. The human PRR2 gene, related to the poliovirus receptor gene (PVR), is the true homolog of the murine MPH gene. *Gene.* 159:267–272.

Edelman, G.M. 1986. Cell adhesion molecules in the regulation of animal form and tissue pattern. *Annu. Rev. Cell Biol.* 2:81–116.

Edelman, G.M., and K.L. Crossin. 1991. Cell adhesion molecules: implications for a molecular histology. *Annu. Rev. Biochem.* 60:155–190.

Furuse, M., T. Hirase, M. Itoh, A. Nagafuchi, S. Yonemura, Sa. Tsukita, and Sh. Tsukita. 1993. Occludin: a novel integral membrane protein localizing at tight junctions. *J. Cell Biol.* 123:1777–1788.

Furuse, M., K. Fujita, T. Hiiragi, K. Fujimoto, and Sh. Tsukita. 1998. Claudin-1 and -2: novel integral membrane proteins localizing at tight junctions with no sequence similarity to occludin. *J. Cell Biol.* 141:1539–1550.

Geiger, B., and D. Ginsberg. 1991. The cytoplasmic domain of adherens-type junctions. *Cell Motil. Cytoskeleton.* 20:1–6.

Geraghty, R.J., C. Krummenacher, G.H. Cohen, R.J. Eisenberg, and P.G. Spear. 1998. Entry of alphaherpesviruses mediated by poliovirus receptor-related protein 1 and poliovirus receptor. *Science.* 280:1618–1620.

Gumbiner, B.M. 1996. Cell adhesion: the molecular basis of tissue architecture and morphogenesis. *Cell.* 84:345–357.

Hanley, T., and J.P. Merlie. 1991. Transgene detection in unpurified mouse tail DNA by polymerase chain reaction. *Biotechniques.* 10:56.

Herrmann, B.G. 1991. Expression pattern of the *Brachyury* gene in whole-mount *Twis/Twis* mutant embryos. *Development.* 113:913–917.

Hock, B., B. Böhme, T. Karn, T. Yamamoto, K. Kaibuchi, U. Hotrich, S. Holland, T. Pawson, H. Rübsamen-Waigman, and K. Strebhardt. 1998. PDZ-domain–mediated interaction of the Eph-related receptor tyrosine kinase EphB3 and the ras-binding protein AF6 depends on the kinase activity of the receptor. *Proc. Natl. Acad. Sci. USA.* 95:9779–9784.

Itoh, M., A. Nagafuchi, S. Yonemura, T. Kitani-Yasuda, Sa. Tsukita, and Sh. Tsukita. 1993. The 220-kD protein colocalizing with cadherins in non-epithelial cells is identical to ZO-1, a tight junction–associated protein in epithelial cells: cDNA cloning and immunoelectron microscopy. *J. Cell Biol.* 121:491–502.

Itoh, M., A. Nagafuchi, S. Moroi, and Sh. Tsukita. 1997. Involvement of ZO-1 in cadherin-based cell adhesion through its direct binding to α catenin and actin filaments. *J. Cell Biol.* 138:181–192.

Kataoka, H., N. Takakura, S. Nishikawa, K. Tsuchida, H. Kodama, T. Kunisada, W. Risau, T. Kita, and S.I. Nishikawa. 1997. Expression of *PDGF receptor alpha, c-Kit* and *Flk1* gene clustering in mouse chromosome 5 define distinct subsets of nascent mesodermal cells. *Dev. Growth Differ.* 39: 729–740.

Kaufman, M.H. 1995. The Atlas of Mouse Development. Revised ed. Academic Press Ltd., London.

Knudsen, K.A., A.P. Soler, K.R. Johnson, and M.J. Wheelock. 1995. Interaction of α-actinin with the cadherin/catenin cell–cell adhesion complex via α-catenin. *J. Cell Biol.* 130:67–77.

Koera, K., K. Nakamura, K. Nakano, J. Miyoshi, K. Toyoshima, T. Hatta, H. Otani, A. Aiba, and M. Katsuki. 1997. K-ras is essential for the development of the mouse embryo. *Oncogene.* 15:1151–1159.

Laemmli, U.K. 1970. Cleavage of structural proteins during the assembly of the head of bacteriophage T4. *Nature.* 227:680–685.

Lopez, M., F. Eberlé, M.G. Mattei, J. Gabert, F. Birg, F. Birdin, C. Maroc, and P. Dubreuil. 1995. Complementary DNA characterization and chromosomal localization of a human gene related to the poliovirus receptor-encoding gene. *Gene.* 155:261–265.

Mandai, K., H. Nakanishi, A. Satoh, H. Obaishi, M. Wada, H. Nishioka, M. Itoh, A. Mizoguchi, T. Aoki, T. Fujimoto, et al. 1997. Afadin: a novel actin filament-binding protein with one PDZ domain localized at cadherin-based cell-to-cell adherens junction. *J. Cell Biol.* 139:517–528.

Mandai, K., H. Nakanishi, A. Satoh, K. Takahashi, K. Satoh, H. Nishioka, A. Mizoguchi, and Y. Takai. 1999. Ponsin/SH3P12: an 1-afadin– and vinculin-binding protein localized at cell–cell and cell-matrix adherens junctions. *J. Cell Biol.* 144:1001–1017.

Morrison, M.E., and V.R. Racaniello. 1992. Molecular cloning and expression of a murine homolog of the human poliovirus receptor gene. *J. Virol.* 66: 2807–2813.

Nagafuchi, A., M. Takeichi, and Sh. Tsukita. 1991. The 102 kd cadherin-associated protein: similarity to vinculin and posttranscriptional regulation of expression. *Cell.* 65:849–857.

Ozawa, M., H. Baribault, and R. Kemler. 1989. The cytoplasmic domain of the cell adhesion molecule uvomorulin associates with three independent proteins structurally related in different species. *EMBO (Eur. Mol. Biol. Organ.) J.* 8:1711–1717.

Prasad, R., Y. Gu, H. Alder, T. Nakamura, O. Canaani, H. Saito, K. Huebner, R.P. Gale, P.C. Nowell, K. Kuriyama, et al. 1993. Cloning of the ALL-1 fusion partner, the AF-6 gene, involved in acute myeloid leukemias with the t(6;11) chromosome translocation. *Cancer Res.* 53:5624–5628.

Rimm, D.L., E.R. Koslov, P. Kebriaei, C.D. Cianci, and J.S. Morrow. 1995. α1(E)-catenin is an actin-binding and -bundling protein mediating the attachment of F-actin to the membrane adhesion complex. *Proc. Natl. Acad. Sci. USA.* 92:8813–8817.

Robertson, E.J. 1987. Embryo-derived stem cell line. *In* Teratocarcinomas and Embryonic Stem Cells: A Practical Approach. E.J. Robertson, editor. IRL Press, Oxford. 71–112.

Rudnicki, M.A., and M.W. McBurney. 1987. Cell culture methods and induction of differentiation of embryonal carcinoma cell line. *In* Teratocarcinomas and Embryonic Stem Cells: A Practical Approach. E.J. Robertson, editor. IRL Press, Oxford. 19–49.

Rudnicki, M.A., T. Braun, S. Hinuma, and R. Jaenisch. 1992. Inactivation of MyoD in mice leads to up-regulation of the myogenic HLH gene Myf-5 and results in apparently normal muscle development. *Cell.* 71:383–390.

Sakisaka, T., H. Nakanishi, K. Takahashi, K. Mandai, M. Miyahara, A. Satoh, K. Takaishi, and Y. Takai. 1999. Different behavior of l-afadin and neurabin-II during the formation and destruction of cell–cell adherens junction. *Oncogene.* 18:1609–1618.

Sambrook, J., E.F. Fritsch, and T. Maniatis. 1989. Molecular Cloning: A Laboratory Manual. 2nd ed. Cold Spring Harbor Laboratory Press, Cold Spring Harbor, NY.

Takahashi, K., H. Nakanishi, M. Miyahara, K. Mandai, K. Satoh, A. Satoh, H. Nishioka, J. Aoki, A. Nomoto, A. Mizoguchi, and Y. Takai. 1999. Nectin/PRR: an immunoglobulin-like cell adhesion molecule recruited to cadherin-based adherens junction through interaction with afadin, a PDZ domain-containing protein. *J. Cell Biol.* 145:539–549.

Takakura, N., H. Yoshida, T. Kunisada, S. Nishikawa, and S.I. Nishikawa. 1996. Involvement of platelet-derived growth factor receptor-alpha in hair canal formation. *J. Investig. Dermatol.* 107:770–777.

Takakura, N., H. Yoshida, Y. Ogura, H. Kataoka, S. Nishikawa, and S.I. Nishikawa. 1997. PDGFRα expression during mouse embryogenesis: immunolocalization analyzed by whole-mount immunohistostaining using the monoclonal anti-mouse PDGFRα antibody APA5. *J. Histochem. Cytochem.* 45: 883–893.

Takeichi, M. 1988. The cadherins: cell–cell adhesion molecules controlling animal morphogenesis. *Development.* 102:639–655.

Takeichi, M. 1991. Cadherin cell adhesion receptors as a morphogenetic regulator. *Science.* 251:1451–1455.

Takeichi, M. 1993. Cadherins in cancer: implications for invasion and metastasis. *Curr. Opin. Cell Biol.* 5:806–811.

Thomas, K.R., and M.R. Capecchi. 1987. Site-directed mutagenesis by gene targeting in mouse embryo-derived stem cells. *Cell.* 51:503–512.

Tsukita, Sh., Sa. Tsukita, A. Nagafuchi, and S. Yonemura. 1992. Molecular linkage between cadherins and actin filaments in cell–cell adherens junctions. *Curr. Opin. Cell Biol.* 4:834–839.

Tucker, K.L., Y. Wang, J. Dausman, and R. Jaenisch. 1997. A transgenic mouse strain expressing four drug-selectable marker genes. *Nucleic Acids Res.* 25:

3745–3746.
Walsh, F.S., and P. Doherty. 1997. Neural cell adhesion molecules of the immunoglobulin superfamily: role in axon growth and guidance. *Annu. Rev. Cell Dev. Biol.* 13:425–456.
Warner, M.S., R.J. Geraghty, W.M. Martinez, R.I. Montgomery, J.C. Whitbeck, R. Xu, R.J. Eisenberg, G.H. Cohen, and P.G. Spear. 1998. A cell surface protein with herpesvirus entry activity (HveB) confers susceptibility to infection by mutants of herpes simplex virus type 1, herpes simplex virus type 2, and pseudorabies virus. *Virology.* 246:179–189.
Weiss, E.E., M. Kroemker, A.-H. Rüdiger, B.M. Jockusch, and M. Rüdiger. 1998. Vinculin is part of the cadherin–catenin junctional complex: complex formation between α-catenin and vinculin. *J. Cell Biol.* 141:755–764.
Wilkinson, D.G. 1992. Whole mount in situ hybridization of vertebrate embryos. *In* In Situ Hybridization: A Practical Approach. D.G. Wilkinson, editor. IRL Press, Oxford, UK. 75–83.
Wilkinson, D.G., S. Bhatt, and B.G. Harrmann. 1990. Expression pattern of the mouse *T* gene and its role in mesoderm formation. *Nature.* 343:657–659.
Williams, A.F., and A.N. Barclay. 1988. The immunoglobulin superfamily—domains for cell surface recognition. *Annu. Rev. Immunol.* 6:381–405.
Yagi, T., Y. Ikawa, K. Yoshida, Y. Shigetani, N. Takeda, I. Mabuchi, T. Yamamoto, and S. Aizawa. 1990. Homologous recombination at c-fyn locus of mouse embryonic stem cells with use of diphtheria toxin A-fragment gene in negative selection. *Proc. Natl. Acad. Sci. USA.* 87:9918–9922.